Publication P3

Kanerva, S., Seman, S., Arkkio, A. 2005. "Inductance Model for Coupling Finite Element Analysis with Circuit Simulation", *IEEE Transaction on Magnetics*, Vol. 41, Issue 5, May 2005, pp. 1620-1623.

Inductance Model for Coupling Finite Element Analysis With Circuit Simulation

Sami Kanerva, Slavomir Seman, *Student Member, IEEE*, and Antero Arkkio

Laboratory of Electromechanics, Helsinki University of Technology, FI-02015 HUT, Finland

This paper presents a method for coupling magnetic field equations of the electrical machine with circuit equations of the windings and external electric circuits. The electrical machine is modeled by the electromotive force and the dynamic inductance, which are determined by finite element method (FEM) and updated at each time step in transient simulation. The external circuit model is simulated in system simulation software, using the parameters obtained by FEM. The method is verified by simulating a doubly fed induction generator in steady state and three-phase short circuit, and comparing the results with those obtained by directly coupled field-circuit simulation. Transient simulation of the generator with a frequency converter and closed-loop control during network disturbance is presented as an example, showing that the method is applicable also for complex systems.

Index Terms—Electric machines, electromagnetic coupling, finite element methods (FEM), inductance, power system simulation.

I. INTRODUCTION

ACCURATE modeling of electrical machines requires simultaneous solution of the finite element method (FEM) equations and circuit equations of the windings [1], [2]. When electrical machines are connected to external circuits, additional circuit equations are also coupled into the system. When complex circuit models are involved, however, direct coupling of all the equations is not a very practical approach because each different case requires programming of a completely new set of equations. To simplify the coupling, methods for automated construction of circuit equations have been developed [3], [4], but any closed-loop control systems cannot be implemented by such methods.

Inclusion of closed-loop control in directly coupled system equations would require enormous work, but using indirect coupling between the FEM model and the external circuit model gives more freedom to construct and modify different parts of the system independently. Reference [5] presents an indirect procedure, where the electrical machine model is solved separately from external circuit model and the results are passed between the field and circuit models with one time-step delay. The circuit model can be implemented in a system simulator and time steps of different length can be used in FEM computation and circuit simulation.

In such a method, output from the FEM model is updated at major time steps only. Hence, the current and voltage waveforms are not continuous at minor time steps used in circuit simulation, which may introduce problems with circuit models containing inductive or capacitive components.

In this paper, we present an indirect method exchanging circuit parameters between FEM and circuit models instead of passing voltage and current waveforms directly. This integrates the FEM model more closely to the circuit model and eliminates the problems with continuity, but still keeps FEM and circuit models separated from each other.

II. COMPUTATIONAL METHODS

A. Finite Element Model of the Electrical Machine

The FEM computation is based on two-dimensional vector potential formulation coupled with the voltage equations of the windings [1]. The magnetic vector potential A satisfies

$$-\nabla \cdot (\nu \nabla A) = J \tag{1}$$

where ν is the nonlinear reluctivity. The current density J is determined by

$$J = \frac{Ni}{S} \tag{2}$$

in a phase winding with cross section area S and N filaments carrying the current i, and

$$J = -\sigma \frac{\partial A}{\partial t} + \sigma \frac{u_{\mathrm{b}}}{l_{\mathrm{b}}} \tag{3}$$

in rotor bars or other solid conductors with conductivity σ. The voltage drop over the conductor and the length of the conductor are denoted by u and l, respectively.

The voltage equations for the phase windings and rotor bars are in the form

$$u = \frac{\mathrm{d}\psi}{\mathrm{d}t} + Ri + L_{\mathrm{e}} \frac{\mathrm{d}i}{\mathrm{d}t} \tag{4}$$

where R is the total resistance of the coil and L_{e} is the additional end-winding inductance. The flux linkage ψ is determined by adding together the contributions of all coil sides in the winding

$$\psi = \sum_{k=1}^{n_{\mathrm{c}}} \beta_k A_k^{\mathrm{ave}} l_k \tag{5}$$

where n_{c} is the total number of coil sides in the winding, β_k is either positive or negative multiplier according to the orientation of the coil side k, A_k^{ave} is the average vector potential, and l_k is the length of the coil side k.

The sources of the field analysis are the voltages applied in the phase windings, which can be located in stator or rotor. For a

cage winding, no additional inputs are required due to the short-circuit ring connecting the bars to each other.

B. Dynamic Inductance Approach

When the flux linkage of a phase winding is defined as a product of inductance L and current i, we obtain the voltage equation of an electrical machine by differentiating the flux with respect to the current and rotor angle θ

$$\frac{\mathrm{d}(Li)}{\mathrm{d}t} = \left(L + \frac{\partial L}{\partial i}i\right)\frac{\partial i}{\partial t} + \left(\frac{\partial L}{\partial \theta}i + L\frac{\partial i}{\partial \theta}\right)\frac{\partial \theta}{\partial t}. \quad (6)$$

From components multiplying the current derivative, we get the dynamic inductance L^{dyn} to represent the total effect of current, including saturation [6]. Position-related components can be considered as the electromotive force e, which comprises saliency, slotting, and coordinate transformations.

For all phase windings, the parameters can be defined as a matrix $\boldsymbol{L}^{\mathrm{dyn}}$ and a vector $\boldsymbol{e}$. Together with the coil resistance matrix $\boldsymbol{R}$, the voltage equation of the electrical machine is

$$\boldsymbol{u} = \boldsymbol{R}i + \boldsymbol{L}^{\mathrm{dyn}}\frac{\mathrm{d}\boldsymbol{i}}{\mathrm{d}t} + \boldsymbol{e} \quad (7)$$

where $\boldsymbol{u}$ and $\boldsymbol{i}$ are vectors comprising the voltages and currents for the phase windings.

In doubly fed machines, the phase windings are located in both stator and rotor. In such cases, $\boldsymbol{u}$ and $\boldsymbol{i}$ are referred in their own coordinate systems corresponding to the real values acting on the windings. Therefore, the cross-coupling between stator and rotor is not present as mutual inductance in $\boldsymbol{L}^{\mathrm{dyn}}$, but it is included in $\boldsymbol{e}$ instead.

C. Extraction of Parameters

After resolving the operating point by the nonlinear field analysis, we linearize the model by fixing the reluctivity values at each element. The circuit parameters $\boldsymbol{L}^{\mathrm{dyn}}$ and $\boldsymbol{e}$ are extracted from the linearized field solution at each time step and passed to the circuit simulator, in which we couple (7) with the external circuit model. It is possible to use shorter time steps in the circuit simulation than in the FEM analysis. In such a case, the circuit parameters are constant until the next time step occurs in the FEM computation.

1) Dynamic Inductance: Based on (6), we define the dynamic inductance as a derivative of the flux linkage with respect to the current. After linearizing the model, we apply small current perturbations Δi separately for each phase winding and calculate the resulting changes in the magnetic flux linkage $\Delta\psi$ for all phases using (5). As a result, we get

$$L_{ij}^{\mathrm{dyn}} = \frac{\Delta\psi_i}{\Delta i_j} \quad (8)$$

for the dynamic inductance between phases i and j. For doubly fed machines, the procedure is applied separately for stator and rotor. Because of the linearized system, the selected value of Δi_j does not affect to the calculated values of L_{ij}^{dyn}.

2) Electromotive Force: Using similar approach as above, we found determining the flux derivative versus rotor position

TABLE I
RATINGS OF THE DOUBLY FED GENERATOR

P_{N}	rated power	1.7 MW
$U_{\mathrm{N,s}}$	rated stator voltage	690 V (delta)
$U_{\mathrm{N,r}}$	maximum rotor voltage[1]	2472 V (star)
f_{N}	rated stator frequency	50 Hz
n_{N}	nominal speed	1500 rpm

[1] In normal use rotor voltage is proportional to slip.

too inaccurate and dependent on the speed and step size. Therefore, we use the dynamic inductance to determine the electromotive force. For the flux linkage vector $\boldsymbol{\psi}$ we have

$$\boldsymbol{e} = \frac{\mathrm{d}\boldsymbol{\psi}}{\mathrm{d}t} - \boldsymbol{L}^{\mathrm{dyn}}\frac{\mathrm{d}\boldsymbol{i}}{\mathrm{d}t} \quad (9)$$

in which we use values from successive time steps to approximate the derivatives. As a result, we obtain the electromotive force for phase i from

$$e_i = \frac{\psi_i(t) - \psi_i(t_0)}{t - t_0} - \sum_{k=1}^{n_{\mathrm{p}}} L_{ik}^{\mathrm{dyn}} \cdot \frac{i_k(t) - i_k(t_0)}{t - t_0} \quad (10)$$

where i, j, and k refer to phase windings, n_{p} is the number of phases, t is the simulation time, and t_0 is the simulation time at previous time step.

D. Implementation for the System Simulation Software

The computational methods were implemented for Simulink using dynamically linked program code (S-function), which is treated as an external function. This function resolves the circuit parameters $\boldsymbol{L}^{\mathrm{dyn}}$ and $\boldsymbol{e}$ from the phase voltages, using finite element analysis. The phase currents are integrated from

$$\frac{\mathrm{d}\boldsymbol{i}}{\mathrm{d}t} = [\boldsymbol{L}^{\mathrm{dyn}}]^{-1}(\boldsymbol{u} - \boldsymbol{e} - \boldsymbol{R}i) - \alpha\boldsymbol{i} \quad (11)$$

where α is the cutoff frequency of a high-pass filter used for drift compensation. For a long simulation, accumulation of small numerical errors may cause drifting in the integrand, which can be prevented by adding the compensation term in the feedback path. In steady-state simulation, an appropriate value for α is 5%–10% of the fundamental angular frequency. When simulating transients, compensation is not used, because it would prevent the dc component from appearing in the current.

III. VERIFICATION

A. Model of the Doubly Fed Induction Generator

We modeled a four-pole 1.7-MW doubly fed induction generator, which has three phases in stator and rotor. Ratings of the generator are presented in Table I and the geometry of the generator model is presented in Fig. 1.

Besides the above methodology with circuit parameters, we also simulated the generator using direct coupling between the field and circuit equations in order to verify the presented method. In both methods, the finite element mesh comprised 949 nodes and 1848 elements. We decided to use first-order elements, since there was no significant difference in results compared with second-order elements. Because of symmetry,
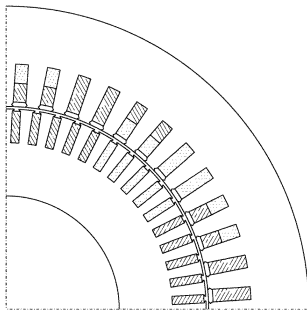
Fig. 1. Geometry of the finite element model. Only one quarter of the cross section is modeled because of symmetry.
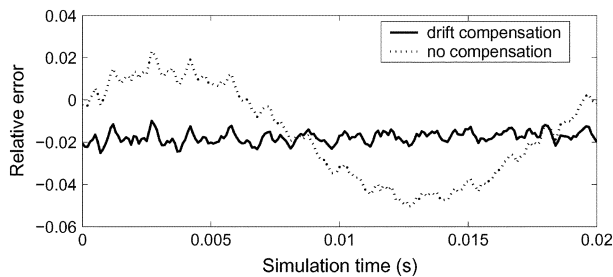

Fig. 2. Relative difference in the stator current, when steady-state simulation results were compared with the results obtained by direct coupling.

the finite element model covers only one quarter of the cross section. Both stator and rotor coils are modeled as phase windings without eddy currents.

B. Simulation Results

We simulated the generator in steady state using sinusoidal supply voltage in stator and rotor. In the simulations, we used 50-Hz stator frequency, 1.7-MW mechanical power, and -10% or -50% slip. The stator voltage was 690 V, and rotor voltage was 240 V for -10% slip and 1250 V for -50% slip. We compared the results with directly coupled simulation, where the phase currents were solved simultaneously with the field equations using uniform time steps. Length of the time step was 100 μs for FEM computation and 10 μs for the circuit simulation. We used drift compensation $\alpha = 15$ rad/s for stator current and no compensation at all for rotor current.

We determined the space vector of the phase current and calculated both absolute and relative error with respect to direct coupling by comparing the space vector amplitudes. With drift compensation, the relative difference in stator current was only about two percent, whereas it was up to five percent without compensation. Variation of the difference with time is illustrated in Fig. 2. In rotor current, the difference was negligible.

Besides steady state, we also simulated a three-phase short circuit in stator, while the rotor voltage was preserved. The space vector amplitude of stator and rotor currents are presented in Fig. 3. Again, we compared the simulation results with those obtained by direct coupling and calculated the absolute and relative differences. The difference fluctuated between positive and negative values, and the average deviation was about two percent in both sides. In Table II, the average differences during the transient are presented for both steady-state and short-circuit simulation.
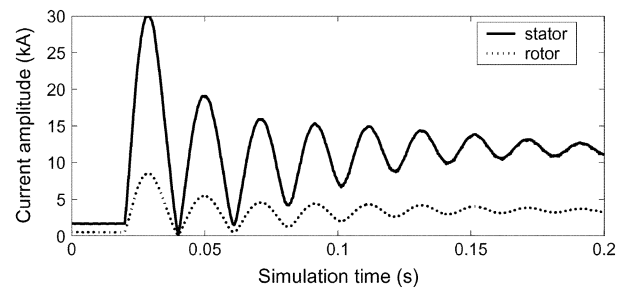

Fig. 3. Space vector amplitude of stator and rotor currents in three-phase short circuit. Rotor voltage was preserved during the fault.

TABLE II
ABSOLUTE AND RELATIVE DIFFERENCES IN SIMULATION RESULTS

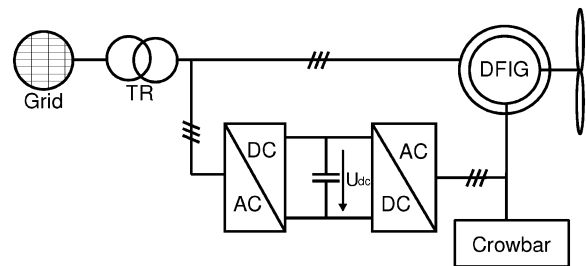|	SLIP = −10%		SLIP = −50%	
STEADY-STATE	abs (A)	rel (%)	abs (A)	rel (%)
stator, α=15	−29	−1.7	−28	−2.6
rotor, α=0	−0.4	−0.1	−2.8	−0.8
SHORT-CIRCUIT	abs (A)	rel (%)	abs (A)	rel (%)
stator, α=0	±180	±2.9	±190	±1.5
rotor, α=0	±40	±2.1	±50	±1.3

Fig. 4. Doubly fed induction generator with frequency converter and crowbar protection in the rotor.

IV. EXAMPLE OF A WIND-POWER APPLICATION

A. Description of the System

As an example, we modeled a wind-power application, where the rotor of the doubly fed induction generator is fed by a frequency converter [7]. The components of the system are presented in Fig. 4. The doubly fed induction generator (DFIG) is modeled by the dynamic inductance and electromotive force, which are embedded into the equivalent circuit of the grid and the transformer (TR). The grid model comprises a sinusoidal voltage source, an inductance, and a resistance in series. The transformer model comprises an inductance and resistance in series, and a parallel capacitance between the phases. The circuit parameters of the generator are calculated by FEM at each major time step (50 μs) and the numerical integration of the circuit model is carried out at minor steps (10 μs).

The frequency converter model comprises two back-to-back connected voltage source inverters and a dc link. The stator-side converter is modeled as a simple first-order filter that controls the dc-link voltage with a PI controller. The rotor side converter is supplied from the common dc link and the switches are assumed to be ideal. The control of the inverter is based on modified direct torque control, where the estimates of flux linkage
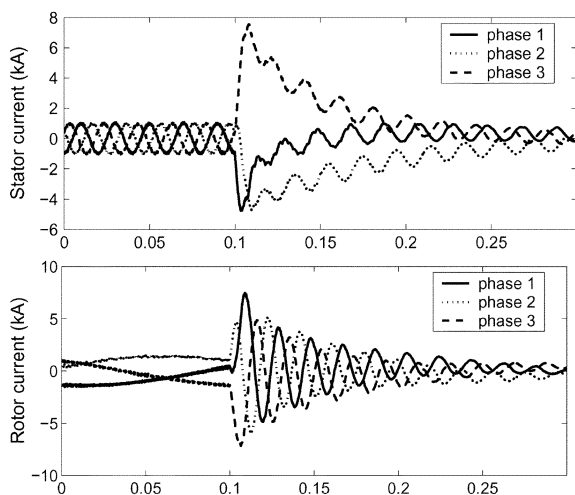
Fig. 5. Stator and rotor currents of the wind generator, when stator voltage drops suddenly to 35% of the rated value.

and torque are calculated from constant equivalent circuit parameters and the currents obtained from the generator model. The crowbar circuit consists of a diode bridge, a resistor, and a thyristor that connects the rectified rotor voltage to the resistor, when the maximum value of the rotor voltage is exceeded.

B. Simulation Results

The system was simulated in normal operation and in fault conditions. In steady state, the mechanical torque was 50% of the rated torque and the speed was 1600 rpm. At time instant $t = 100$ ms, the stator voltage drops suddenly to 35% of the rated value. The control system disconnects the frequency converter and the crowbar starts protecting the rotor circuit. The stator remains connected to the grid during the fault.

The simulated stator and rotor currents are presented in Fig. 5. The results are similar to those obtained earlier using analytical machine models [7], [8], and they show that the method is also applicable to systems with closed-loop control. However, we also observed that the control system is very sensitive to all variation in stator current. As a result, there was slow fluctuation in the torque in steady state, and the average switching frequency in the frequency converter was increased. Therefore, special attention should be paid to selecting the numerical methods for integration.

V. DISCUSSION

Comparison with the directly coupled field-circuit equations shows good agreement, even though some filtering was required in the steady-state simulation to prevent the values from drifting in the numerical integration. This is mostly due to the weak coupling between the parameter calculation and numerical integration of the phase currents. Adding a closed iteration loop between the FEM computation and the system simulator would provide more stable simulation, but the implementation would also be more complex, requiring access also to program code of

the system simulator. Simulation of transients, however, shows good agreement even without filtering. An example case, where a doubly fed induction generator and a frequency converter with direct torque control was simulated, shows that the method is also applicable to complex systems with closed-loop control. The method can be applied in most commercial circuit simulators with an option to import user's own program code, but time consumption of this method is slightly higher than in the directly coupled computation because of the circuit parameter extraction and numerical integration in the circuit simulation.

However, the method is not ideal for all cases with coupled field and circuit equations. For plain impedance in series with the windings, direct coupling with the FEM equations is a simpler approach. For controlled frequency converter supply, there is some problematic interference between parameter variation, numerical integration, and the sensitive control system. Nevertheless, without the grid model, and assuming ideal switches, even weak coupling between the electrical machine model and control system model can be applied successfully [5]. As a conclusion, the presented method is the most beneficial in cases, where the external circuit is relatively complex and consists mostly of passive circuit elements.

REFERENCES

[1] A. Arkkio, "Analysis of induction motors based on the numerical solution of the magnetic field and circuit equations,", [Online] Available: http://lib.hut.fi/Diss/198X/isbn951226076X/, 1987.
[2] S. J. Salon, M. J. DeBortoli, and R. Palma, "Coupling of transient fields, circuits, and motion using finite element analysis," *J. Electromagn. Waves Applicat.*, vol. 4, no. 11, pp. 1077–1106, Nov. 1990.
[3] J. Väänänen, "Circuit theoretical approach to couple two-dimensional finite element models with external circuit connections," *IEEE Trans. Magn.*, vol. 32, no. 2, pp. 400–410, Mar. 1996.
[4] P. Kuo-Peng, N. Sadowski, J. P. A. Bastos, R. Carlson, N. J. Batistela, and M. Lajoie-Mazenc, "A general method for coupling static converters with electromagnetic structures," *IEEE Trans. Magn.*, vol. 33, no. 2, pp. 2004–2009, Mar. 1997.
[5] S. Kanerva, S. Seman, and A. Arkkio, "Simulation of electric drive systems with coupled finite element analysis and system simulator," presented at the 10th Eur. Conf. Power Electronics and Applications EPE 2003, Toulouse, France, Sep. 2003, CD-ROM.
[6] N. A. Demerdash and T. E. Nehl, "Electric machinery parameters and torques by current and energy perturbations from field computation—Part I: Theory and formulation," *IEEE Trans. Energy Convers.*, vol. 14, no. 4, pp. 1507–1513, Dec. 1999.
[7] S. Seman, J. Niiranen, S. Kanerva, and A. Arkkio, "Analysis of a 1.7 MVA doubly fed wind-power induction generator during power systems disturbances," presented at the Nordic Workshop on Power and Industrial Electronics NORPIE, Trondheim, Norway, Jun. 2004, CD-ROM.
[8] J. Niiranen. Voltage dip ride through of doubly fed generator equipped with active crowbar. presented at Nordic Wind Power Conference 2004. [Online]. Available: http://www.elkraft.chalmers.se/NWPC/nwpc.html